

# Scanning tunneling spectroscopy of InAs nanocrystal quantum dots

Oded Millo and David Katz

*Racah Institute of Physics, The Hebrew University, Jerusalem 91904, Israel*

YunWei Cao and Uri Banin\*

*Department of Physical Chemistry and the Farkas Center for Light Induced Processes, The Hebrew University, Jerusalem 91904, Israel*

(Received 6 January 2000)

Scanning tunneling spectroscopy is used to investigate single InAs nanocrystals, 20–70 Å in diameter, in a highly asymmetric double barrier tunnel junction configuration. The  $I$ - $V$  characteristics reflect contributions of both single-electron charging and the atomiclike level structure of the quantum dots. The spectra are simulated and well described within the framework of the ‘‘orthodox model’’ for single-electron tunneling. The peaks in the tunneling spectra display a systematic broadening with the reduction of dot diameter, from 40 to 150 meV over the studied quantum dot size range. This is assigned to a decreased electron dwell time on the dot, due to reduction of the barrier height, induced by the blueshift of the quantum-confined levels. The distribution of peak spacings within charging multiplets in the tunneling spectra is found to be Gaussian, resembling observations on metallic quantum dots.

## INTRODUCTION

The evolution of the electronic structure of semiconductor nanocrystal quantum dots (QD) as a function of size, manifests the transition from the molecular to the solid-state regime.<sup>1</sup> Extensive optical spectroscopy studies of QDs demonstrate their atomlike discrete level structure and ultra narrow transition linewidths.<sup>2–5</sup> The optical spectroscopy probes allowed transitions between the QD valence band (VB) and conduction band (CB) states, and the assignment of the spectrum relied on correlation with theoretical models.<sup>6,7</sup> Tunneling measurements, on the other hand, can probe separately the discrete states in the QD conduction and valence bands thus providing complimentary unique information on the electronic properties of nanocrystals.<sup>8,9</sup> However, only a few works on tunneling spectroscopy of semiconductor nanocrystal QDs were reported so far.<sup>8–10</sup> On the other hand, comprehensive tunneling spectroscopy studies were carried out on metallic QDs, focusing on single-electron charging effects such as the Coulomb blockade and the Coulomb staircase.<sup>11–14</sup> In these systems, the single-electron charging energy,  $E_c$ , is substantially larger than the level spacing, and the effect of the latter on the tunneling spectra was investigated at sub-Kelvin temperatures.<sup>15–17</sup> Recently, special focus was given to the manifestation of the level structure in the statistics of the peak spacings in the tunneling spectra of various metallic quantum dot systems.<sup>18,19</sup> For dots defined in high mobility, two-dimensional free-electron gas,<sup>18,19</sup> as well as for metal-oxide nanoparticles,<sup>20</sup> the distribution of the peak spacings was found to be Gaussian with a width of  $\sim 0.1E_c$ . This is in contrast to theoretical expectations of a bimodal distribution with a component that follows the Wigner surmise.<sup>21</sup> The bimodal distribution was expected in light of the differences between even and odd electron occupation of the metallic QDs whereas the assumed chaotic nature of the dot would lead to the Wigner distribution of the QD energy-level spacing.

In the present paper we investigate semiconductor QDs.

For an InAs nanocrystal, 5 nm in diameter, the single-electron charging energy is estimated to be  $\sim 0.2$  eV, on the order of or smaller than the typical discrete energy-level spacings. This presents an interesting regime for single charge tunneling, substantially different from the nanometer size metallic islands. In this case, the level structure has a dominant signature in the tunneling spectra. Nevertheless, we find surprising similarities in the behavior of the InAs QDs and the metallic systems.

In a recent publication,<sup>8</sup> we reported on correlation of scanning tunneling spectroscopy and optical spectroscopy of InAs QDs. Two and up to sixfold charging multiplets in the tunneling spectra, were assigned to tunneling through discrete QD states with atomiclike  $s$  and  $p$  symmetries, identified as the  $1S_e$  and  $1P_e$  CB states. The behavior of electron tunneling through the QD states resembles the *Aufbau* (buildup) principle of electron occupation in atoms. Surprisingly, good correlation was found between optical transitions and spacing of levels detected in the tunneling spectra. This unique correlation enabled us to directly deduce information about the symmetry of the ground and first excited state of the complex QD VB.

In this paper, we present a detailed analysis of these tunneling spectra. The data are described and simulated using the orthodox model for single-electron tunneling.<sup>11,12</sup> The peak widths in the tunneling spectra are significantly larger than optical transition linewidths, and are broadened with reduced QD size. This behavior is attributed to the short dwell time of the electrons on the nanocrystal. Finally, we analyze the statistics of peak spacing in the tunneling spectra, which shows a similar behavior to that observed for metallic QDs.

## EXPERIMENT

Crystalline InAs QDs were prepared using a solution phase pyrolytic reaction of organometallic precursors. These nanocrystals are nearly spherical in shape with size con-

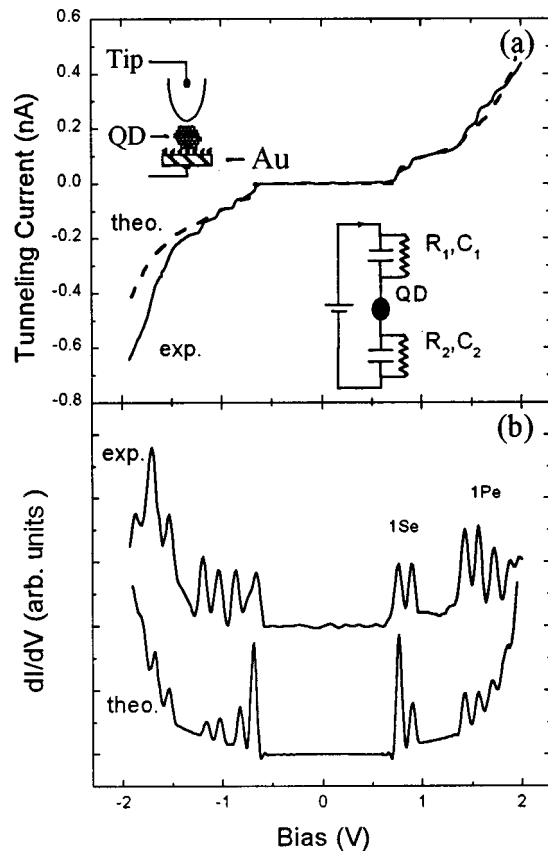


FIG. 1. Tunneling spectroscopy of a single InAs nanocrystal, 22 Å in radius ( $T=4.2$  K). (a) Measured  $I$ - $V$  curve (solid line) and the simulated one (dotted line). The DBTJ configuration and the equivalent circuit are shown schematically in the insets. (b) Simulated (bottom trace) and experimental tunneling conductance spectra.

trolled between 10–40 Å in radius, and 10% size distributions.<sup>3,22</sup> The nanocrystal surface is passivated by organic ligands. For the tunneling measurements we link the nanocrystals to a gold film via hexane dithiol molecules,<sup>23</sup> as shown schematically in the upper inset of Fig. 1(a).

Scanning tunneling microscopy (STM) data were obtained using a homebuilt cryogenic STM. The scan head and sample area are evacuated just before introducing helium exchange gas and inserting the STM to the liquid helium bath. All data presented here were acquired at 4.2 K. In a typical experiment, a topographic image of an isolated InAs QD was taken, from which its size was determined.<sup>8</sup> Then, the STM tip was positioned above the QD, forming a double barrier tunnel junction (DBTJ) configuration,<sup>11,12</sup> as depicted in Fig. 1(a). Tunneling  $I$ - $V$  or  $dI/dV$  versus  $V$  characteristics were acquired while disabling the scanning and feedback controls. These data were acquired with the tip retracted from the QD to a distance where the bias predominantly drops on the tip-QD junction, forming a highly asymmetric DBTJ. In these conditions, CB (VB) states appear at positive (negative) sample bias, and the real QD level separations can be extracted directly from the peak spacings.<sup>8,24</sup>

## RESULTS AND DISCUSSION

The  $I$ - $V$  curve in Fig. 1(a) was acquired on an InAs QD, 22 Å in radius. This curve, typical of others, shows a region

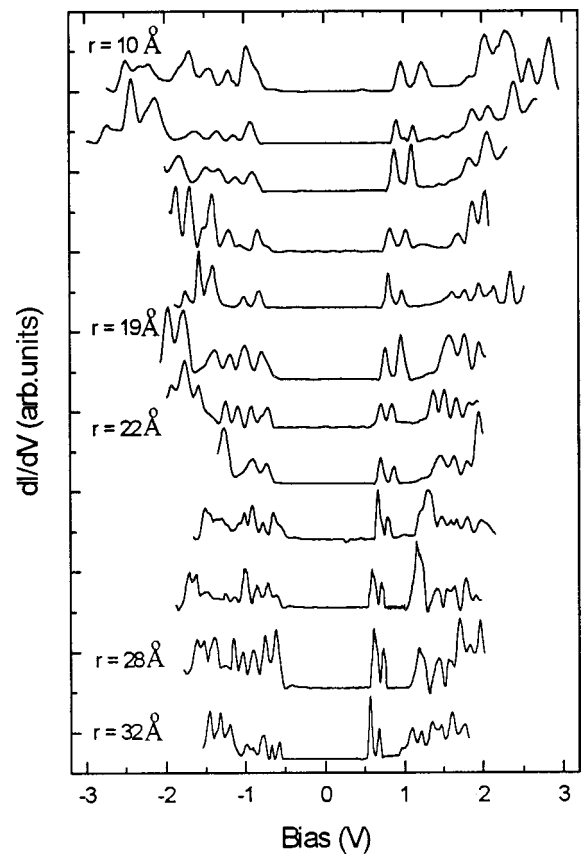


FIG. 2. Size evolution of the tunneling  $dI/dV$  vs  $V$  characteristics of single InAs QDs displaced vertically for clarity. The position of the centers of the zero current gap showed nonsystematic variations with respect to the zero bias, of the order of 0.2 eV, probably due to variations of local offset potentials. For clarity of presentation, we offset the spectra along the  $V$  direction to center them at zero bias. Representative nanocrystal radii are denoted. All spectra were acquired at  $T=4.2$  K.

of suppressed tunneling current around zero bias, followed by a series of steps at both negative and positive bias. In Fig. 1(b) we present the corresponding  $dI/dV$  versus  $V$ , tunneling conductance spectrum, which is proportional to the tunneling density-of-states.<sup>25</sup> A series of discrete peaks is clearly observed, where the separations are determined by both the single-electron charging energy and the discrete level spacings in the QD. Also presented in the figure is a fit to the orthodox model for single-electron tunneling, which will be discussed below.

In Fig. 2, we plot a set of tunneling-conductance spectra acquired on InAs QDs of radii ranging from 35–10 Å. In Ref. 8, we discussed the detailed assignment of the observed peaks, and extracted spectroscopic information from these data. Briefly, on the positive bias side, immediately following current onset, we always observed a doublet that we assign to tunneling through the twofold spin degenerate  $1S_e$  CB state. Then, a larger spacing is observed followed by a higher multiplet, of up to six peaks, that we attribute to the CB  $1P_e$  state. The negative bias side shows a more complex structure, reflecting the complicated QD VB level spectrum,<sup>3</sup> but in each spectra one can identify two peaks with a larger separation, from which the spacing between the ground and first excited VB levels was extracted.

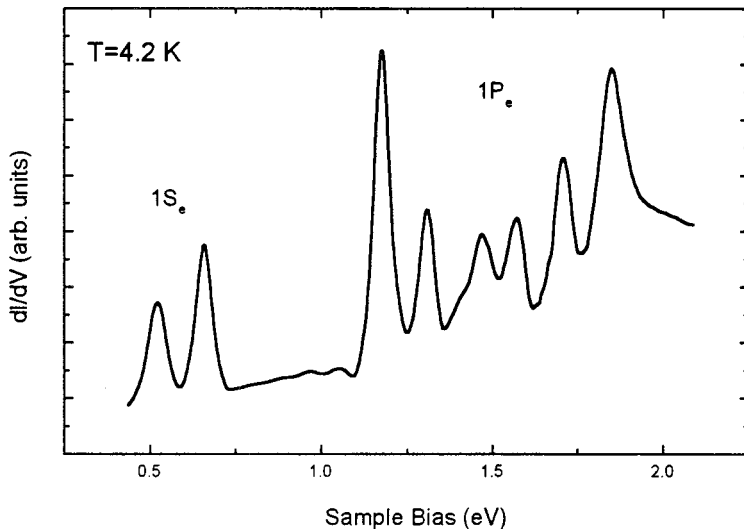


FIG. 3. A tunneling conductance spectrum (positive bias side), measured for an InAs QD with radius of 28 Å using a lock-in technique. A doublet and a sixfold multiplet are resolved, assigned to tunneling through the  $1S_e$  and  $1P_e$  QD states, respectively.

The  $dI/dV$  curves presented in Fig. 2 are numerical derivatives of the measured  $I-V$  curves. The voltage range in each spectrum is limited by the onset of field emission and the saturation of the current preamplifier. A direct measurement of a tunneling-conductance spectrum (positive bias side) using a lock-in technique, for a QD 28 Å in radius, is presented in Fig. 3. The data acquisition time is long in this case, but the increased sensitivity allows the measurement to be carried out at lower tunneling currents (larger tip-sample separation), delaying field emission and preamplifier saturation to larger bias. In this case, we exactly resolve a sixfold multiplet in the second group of peaks. We also note, that the spectra obtained from the direct lock-in method are similar, in the peak spacings and widths, to those obtained by numerical derivation of the measured  $I-V$  characteristics. From the peak spacings within the multiplets, we extracted the charging energy  $E_c$  while the intermultiplet peak spacing is the sum of the corresponding level spacing (this includes the band gap  $E_g$ ) and  $E_c$ .

This picture, in which the tunneling conductance curves of the QDs are described as a simple sum of level spacing and charging energy, is supported by our theoretical simulations. We calculated the spectra using the “orthodox model” for single-electron tunneling,<sup>11</sup> modified to account for the discrete QD level spectrum,<sup>24</sup> as shown in Fig. 1. The starting point of this simulation is an assumed QD level structure consisting of two CB and two VB states. The spacings and degeneracy of these states were inferred from the measured tunneling data and the good correlation with the optical spectra. Accordingly, the first CB state was taken to be twofold degenerate, while the second state was sixfold degenerate. Both ground and excited VB states were taken to be fourfold degenerate. Each tunnel barrier is characterized by two parameters—a tunneling resistance  $R_i$ , and a capacitance  $C_i$ , where  $i=1,2$  for the tip-QD and QD-gold junctions, respectively. The peak positions are not sensitive to the resistance values,<sup>11</sup> and are determined primarily by  $C_1$  and  $C_2$ . Good agreement with the experimental peak positions was obtained using values of 0.1 and 1.1 aF, respectively [Fig. 1(b)]. These capacitances set  $E_c$  and the voltage division between the two junctions; most of the bias indeed falls on the tip-QD junction. The asymmetry of the DBTJ is also reflected in the tunneling resistance values. The current is

governed by junction 1, and from the  $I$  and  $V$  settings prior to acquisition of the tunneling spectrum we obtain  $R_1 \sim 10^{10} \Omega$ .  $R_1$  determines the slope on a step, which is also well reproduced in the simulation [Fig. 1(a)].  $R_2$  affects mainly the width of the peaks, from which a value  $\sim 10^5 \Omega$  is found, as shown below. The extracted junction parameters reflect the pronounced asymmetry that we have realized in the DBTJ. This asymmetry is due both to our procedure of tip retraction, and to the dielectric constant and transport properties of the hexane dithiol layer, which lead to formation of a strong tunnel barrier between the tip and the QD, and a weak barrier between the QD and the gold substrate.

Due to this asymmetric configuration, the electron dwell time on the QD is determined by the QD-gold junction. We suggest that this dwell time determines the tunneling peak width, and is the source of the systematic broadening of the peaks in smaller QDs (see Fig. 2). We investigate this conjecture for the  $1S_e$  doublet, which was consistently well resolved in all spectra. Figure 4 shows the size dependence of these peak widths. We determine the width by a fit, as demonstrated in the lower inset. The widths range from approxi-

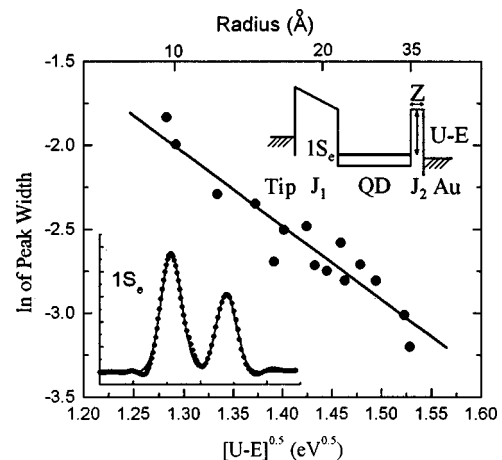


FIG. 4. Size dependence of the average peak width in the  $1S_e$  doublet. The width was extracted by a fit, as depicted in the lower inset for one representative doublet. The upper inset schematically depicts our model for the highly asymmetric DBTJ. The solid line is a least-square linear fit to the data. See text for details.

mately 40 meV for a QD with a radius of 35 Å up to 150 meV for a QD with a radius of 10 Å, significantly larger than typically observed in tunneling experiments on metallic QDs.<sup>15</sup>

The peak widths are well above our experimental resolution and are also substantially larger than  $K_B T$ . They are significantly broadened compared to homogeneous linewidths measured for the lowest optical excitonic transition in isolated nanocrystal systems, using hole burning or photon echoes.<sup>26,27</sup> Therefore, the tunneling peak widths cannot reflect an intrinsic property of the isolated QD, but rather the dwell time of electrons tunneling through the QD. This dwell time is determined by the tunneling rate  $\Gamma_2$  through the weak QD-gold tunnel junction ( $J_2$  in the inset of Fig. 4).  $\Gamma_2$  is related to the tunneling resistance  $R_2$  by  $\Gamma_2 = V_2 / eR_2$ , where  $V_2$  is the voltage drop on the junction. From the typical width  $\Delta E$  of the  $1S_e$  tunneling peaks, using the uncertainty relation  $\Delta E = \hbar \Gamma_2$ , we can estimate the value of  $R_2 \sim 10^5 \Omega$ , only slightly higher than the quantum resistance  $h/e^2$ .

To further establish the feasibility of this picture, we write an expression for  $\Gamma_2$ , assuming a simple square geometry for the tunnel junction  $J_2$ ,<sup>28</sup>

$$\ln \Gamma_2 \propto -2z/\hbar \sqrt{2m_e(U-E)}, \quad (1)$$

where  $z$  is the barrier width,  $m_e$  is the electron mass,  $U$  is the depth of the CB spherical well, and  $E$  the energy of the  $1S_e$  level (see inset of Fig. 4).  $z$  is similar for all QD sizes since we always used the same linker molecule to connect the nanocrystals to the gold substrate. Thus, the sole size dependent part of Eq. (1) comes from the variation of the tunneling barrier height,  $U-E$ . This barrier is systematically reduced in smaller nanocrystals because of the increase in  $E$  due to quantum confinement, while  $U$  remains constant. We calculated the confinement energies of the electron and hole in InAs QDs using an effective-mass model of a spherical well with a finite barrier,<sup>29</sup> with  $U$  as the free parameter. By fitting the calculated values to the size dependence of the band gap  $E_g$ , extracted from the tunneling measurements, we obtained a value of 2.8 eV for  $U$ , a reasonable number for InAs nanocrystals coated by organic ligands. This calculation also shows that the ratio of the (lighter) electron and (heavier) hole confinement energies, ranges between 1.5 to 3 over our size range. Using these values,  $E$  was determined as the relative fraction of the difference between the measured  $E_g$  and 0.42 eV, the bulk InAs band gap. The data, plotted in Fig. 4 versus  $(U-E)^{0.5}$ , indeed exhibits the trend predicted by Eq. (1). Moreover, the least-square fit presented by the straight line, corresponds to  $z = 5 \text{ \AA}$ , a reasonable value for the linker molecules used in our experiment. This illustrative picture captures the essence of the tunneling process in our DBTJ, in particular the role of the barrier strength in determining the electron dwell time on the dot and consequently the single-electron tunneling peak width. The effect of the barrier strength on the width of single-electron tunneling peaks was previously studied for a DBTJ containing a metallic QD in the regime where the tunneling resistance is on the order of the quantum resistance.<sup>30</sup> A broadening of the peak width with reduced barrier strength was observed, consistent with our observations.

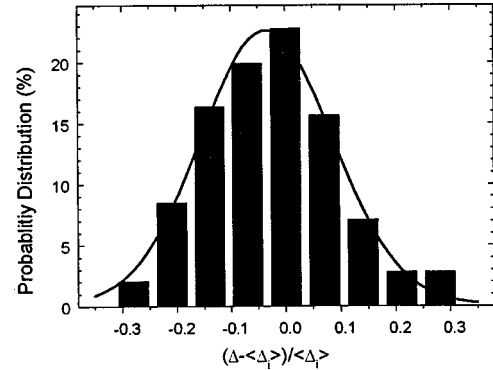


FIG. 5. Histogram of the normalized fluctuations in the peak spacings within charging multiplets, along with a fit to a Gaussian distribution (solid line). The width of the distribution corresponds to  $0.12E_c$ , see text.

An additional question that arises from the tunneling data is related to the statistics of the peak spacings. This issue has recently been studied for two- and three-dimensional metallic QDs having free carriers in their neutral state. Contrary to initial expectations, the spacing distribution was Gaussian with a width that scales with  $E_c$ , and did not follow the Wigner distribution.<sup>18,19</sup> In Fig. 5 we plot a histogram of the normalized peak spacing fluctuation within charging multiplets. The data were accumulated for all QDs taking into account both CB and VB charging multiplets. We followed a normalization procedure similar to that performed in the case of the metallic QDs studied in Refs. 18 and 19. For each dot  $i$ , the intramultiplet spacings  $\Delta$  are presented relative and normalized to the average spacing within the multiplets  $\langle \Delta_i \rangle$ . Recall that we associate  $\langle \Delta_i \rangle$  with the charging energy of the dot  $E_c$ . The distribution is found to be Gaussian, with a width that corresponds to  $0.12E_c$  (see Fig. 5). Interestingly, the shape and width of the distribution observed on our semiconductor nanocrystals, is similar to that observed on the metallic QDs of various types, in spite of the distinct differences between the two systems. This ‘‘universal behavior’’ may result from mesoscopic fluctuations in the charging energy,<sup>18</sup> and further establishes our assignment of the peak multiplets to single-electron charging of degenerate QD states and not to degeneracy lifting. In the latter case, the fluctuations are not expected to scale with the charging energy.

## CONCLUSIONS

Our single-electron tunneling data for InAs nanocrystals, show many features common to those observed for metallic QDs. This is in spite of the distinct differences in the characteristics of the two types of systems: In our semiconducting QDs in contrast to the metallic systems, the level spacings are comparable to or larger than  $E_c$ , and there are no free electrons. Nonetheless, our tunneling data could be well described and simulated as a sum of the QD level spacings and the charging energies—a straightforward extension of the constant interaction, orthodox model, developed for the metallic QDs. The peak widths in our tunneling data are, however, much larger than those observed in previous tunneling experiments. In our highly asymmetric DBTJ measurement configuration, this behavior is attributed to the

weak QD-gold barrier that governs the electron dwell time on the dot. Further investigations of the effect of this tunnel junction on the tunneling characteristics is required. The statistics of peak spacings showed a common behavior to that observed for the metallic dots, manifesting the generality of single-electron tunneling phenomena.

## ACKNOWLEDGMENT

We thank Yair Levi for useful discussions and for his help in the computer simulations. This work was supported by the BICHURA foundation of the Israeli Academy of Sciences and by Intel-Israel.

\*To whom correspondence should be addressed. Electronic address: banin@chem.ch.huji.ac.il

<sup>1</sup>A. P. Alivisatos, *Science* **271**, 933 (1996).

<sup>2</sup>D. J. Norris, A. Sacra, C. B. Murray, and M. G. Bawendi, *Phys. Rev. Lett.* **72**, 2612 (1994); D. J. Norris and M. G. Bawendi, *Phys. Rev. B* **53**, 16 338 (1996).

<sup>3</sup>U. Banin, J. C. Lee, A. A. Guzelian, A. V. Kadavanich, A. P. Alivisatos, W. Jaskolski, G. W. Bryant, Al. L. Efros, and M. Rosen, *J. Chem. Phys.* **109**, 2306 (1998); U. Banin, J. C. Lee, A. A. Guzelian, A. V. Kadavanich, and A. P. Alivisatos, *Superlattices Microstruct.* **22**, 559 (1997).

<sup>4</sup>M. Leon, P. M. Petroff, D. Leonard, and S. Fafard, *Science* **267**, 1966 (1995).

<sup>5</sup>S. A. Empedocles, D. J. Norris, and M. G. Bawendi, *Phys. Rev. Lett.* **77**, 3873 (1996).

<sup>6</sup>A. I. Ekimov, F. Hache, M. C. Schanne-Klein, D. Ricard, C. Flytzanis, I. A. Kudryavtsev, T. V. Yazeva, A. V. Rodina, and A. L. Efros, *J. Opt. Soc. Am. B* **10**, 100 (1993).

<sup>7</sup>H. Fu and A. Zunger, *Phys. Rev. B* **57**, R15 064 (1998); H. Fu, L. W. Wang, and A. Zunger, *Phys. Rev. B* **57**, 9971 (1998).

<sup>8</sup>U. Banin, Y. W. Cao, D. Katz, and O. Millo, *Nature (London)* **400**, 542 (1999).

<sup>9</sup>B. Alpers, G. Hodes, I. Rubinstein, D. Porath, and O. Millo, *Appl. Phys. Lett.* **75**, 1751 (1999).

<sup>10</sup>D. L. Klein, R. Roth, A. K. L. Lim, A. P. Alivisatos, and P. L. McEuen, *Nature (London)* **389**, 699 (1997); D. L. Klein, P. L. McEuen, J. E. Bowen Katari, R. Roth, and A. P. Alivisatos, *Appl. Phys. Lett.* **68**, 2574 (1996).

<sup>11</sup>A. E. Hanna and M. Tinkham, *Phys. Rev. B* **44**, 5919 (1991).

<sup>12</sup>*Single Charge Tunneling*, edited by H. Grabert and M. H. Devoret (Plenum, New York, 1992).

<sup>13</sup>E. Bar-Sadeh, Y. Goldstein, B. Abeles, and O. Millo, *Phys. Rev. B* **50**, R8961 (1994).

<sup>14</sup>C. Schonenberg, H. van Houten, and H. C. Donkersloot, *Europhys. Lett.* **20**, 249 (1992).

<sup>15</sup>D. C. Ralph, C. T. Black, and M. Tinkham, *Phys. Rev. Lett.* **74**, 3241 (1995).

<sup>16</sup>O. Agam, N. S. Wingreen, B. L. Altshuler, D. C. Ralph, and M. Tinkham, *Phys. Rev. Lett.* **78**, 1956 (1997).

<sup>17</sup>J. G. A. Dubois, J. W. Gerritsen, S. E. Shafranjuk, E. J. G. Boon, G. Schmid, and H. van Kempen, *Europhys. Lett.* **33**, 279 (1995).

<sup>18</sup>U. Sivan, R. Berkovits, Y. Aloni, O. Prus, A. Auerbach, and G. Ben-Yoseph, *Phys. Rev. Lett.* **77**, 1123 (1996); R. Berkovits, *ibid.* **81**, 2128 (1998).

<sup>19</sup>S. R. Patel, S. M. Cronenwett, D. R. Stewart, A. G. Huibers, C. M. Marcus, C. I. Duruöz, J. S. Harris, Jr., K. Campman, and A. C. Gossard, *Phys. Rev. Lett.* **80**, 4522 (1998).

<sup>20</sup>V. Chandrashekar and R. A. Webb, *J. Low Temp. Phys.* **97**, 9 (1994).

<sup>21</sup>M. L. Mheta, *Random Matrices* (Academic, New York, 1967).

<sup>22</sup>A. A. Guzelian, U. Banin, A. V. Kadavanich, X. Peng, and A. P. Alivisatos, *Appl. Phys. Lett.* **69**, 1432 (1996).

<sup>23</sup>V. L. Colvin, A. N. Goldstein, and A. P. Alivisatos, *J. Am. Chem. Soc.* **114**, 5221 (1992).

<sup>24</sup>D. Porath and O. Millo, *J. Appl. Phys.* **81**, 2241 (1997); D. Porath, Y. Levi, M. Tarabiah, and O. Millo, *Phys. Rev. B* **56**, 9829 (1997).

<sup>25</sup>R. Wiesendanger, *Scanning Probe Microscopy and Spectroscopy* (Cambridge University Press, London, 1994).

<sup>26</sup>D. M. Mittleman, R. W. Schoenlein, J. J. Shiang, V. L. Colvin, A. P. Alivisatos, and C. V. Shank, *Phys. Rev. B* **49**, 14 435 (1994).

<sup>27</sup>U. Banin, G. Cerullo, A. A. Guzelian, C. J. Bardeen, A. P. Alivisatos, and C. V. Shank, *Phys. Rev. B* **55**, 7059 (1997).

<sup>28</sup>E. L. Wolf, *Principles of Electron Tunneling Spectroscopy* (Oxford University Press, Oxford, 1989).

<sup>29</sup>D. Schoos, A. Mews, A. Eychmuller, and H. Weller, *Phys. Rev. B* **49**, 17 072 (1994).

<sup>30</sup>P. Joyez, V. Bouchiat, D. Esteve, C. Urbina, and M. H. Devoret, *Phys. Rev. Lett.* **79**, 1349 (1997).